CENTER FOR ADVANCED RESEARCH IN FINANCE
GRADUATE SCHOOL OF ECONOMICS, THE UNIVERSITY OF TOKYO

CARF Working Paper

CARF-F-584

Optimal Vaccine Allocation Strategy: Theory and Application to the Early Stage of COVID-19 in Japan

Toshikazu Kuniya
Graduate School of System Informatics, Kobe University

Taisuke Nakata
Graduate School of Economics and Graduate School of Public Policy, University of Tokyo

Daisuke Fujii
Research Institute of Economy, Trade and Industry

April 26, 2024

CARF is presently supported by Nomura Holdings, Inc., Mitsubishi UFJ Financial Group, Inc., Sumitomo Mitsui Banking Corporation., Sumitomo Mitsui Trust Bank, Limited, The University of Tokyo Edge Capital Partners Co., Ltd., Brevan Howard Asset Management LLP, Ernst & Young ShinNihon LLC, SUMITOMO LIFE INSURANCE COMPANY, and All Nippon Asset Management Co., Ltd.. This financial support enables us to issue CARF Working Papers.

Optimal Vaccine Allocation Strategy: Theory and Application to the Early Stage of COVID-19 in Japan[1]

Toshikazu Kuniya[2] **Taisuke Nakata[3]** **Daisuke Fujii[4]**

April 26, 2024

Abstract

We construct an age-structured epidemic model to analyze the optimal vaccine allocation strategy in an epidemic. We focus on two topics: the first one is the optimal vaccination interval between the first and second doses, and the second one is the optimal vaccine allocation ratio between young and elderly people. On the first topic, we show that the optimal interval tends to become longer as the relative efficacy of the first dose to the second dose (RE) increases. On the second topic, we show that the heterogeneity in the age-dependent susceptibility (HS) affects the optimal allocation ratio between young and elderly people, whereas the heterogeneity in the contact frequency among different age groups (HC) tends to affect the effectiveness of the vaccination campaign. A counterfactual simulation suggests that the epidemic wave in the summer of 2021 in Japan could have been greatly mitigated if the optimal vaccine allocation strategy had been taken.

Keywords: COVID-19, Vaccination, SIR Model, Age Structure, Optimal allocation

---

[1] Toshikazu Kuniya is supported by JSPS Grant-in-Aid for Scientific Research (KAKENHI), Project Numbers 19K14594, 23K03214, and JST, PREST Grant Number JPMJPR23R5, Japan. Taisuke Nakata is supported by JSPS Grant-in-Aid for Scientific Research (KAKENHI), Project Number 22H04927, the Research Institute of Science and Technology for Society at the Japan Science and Technology Agency, the Center for Advanced Research in Finance at the University of Tokyo.

[2] Graduate School of System Informatics, Kobe University, 1-1 Rokkodai-cho, Nada-ku, Kobe 657-8501, Japan. tkuniya@port.kobe-u.ac.jp.

[3] Graduate School of Economics and Graduate School of Public Policy, University of Tokyo, 7-3-1, Hongo, Bunkyo-ku, Tokyo 113-0033, Japan. taisuke.nakata@e.u-tokyo.ac.jp

[4] Research Institute of Economy, Trade and Industry, 1-3-1, Kasumigaseki Chiyoda-ku, Tokyo 100-8901, Japan. fujii-daisuke@rieti.go.jp

1. Introduction

In the early stage of the coronavirus disease outbreak 2019 (COVID-19), people had to rely on non-pharmaceutical interventions (NPIs) such as lockdown. Although lockdowns were effective in temporary suppressing the epidemic [1], they brought serious damages to the socio-economic systems in many countries [2]. Vaccination is thought to be one of the most cost-effective pharmaceutical interventions and is often regarded as a game-changer that returned our lives to less restrictive ones.

In the early stage of COVID-19, the amount of available vaccines was limited in many countries. Hence, designing how to allocate them from the viewpoint of minimizing the epidemic damage was important [3]. To design the optimal vaccine allocation, one can consider two ways of optimization: the first one is to optimize the interval between the first and second doses, and the second one is to optimize the ratio of allocation among different age groups. In this study, we deal with these two optimization problems by using a mathematical model, and construct a general theoretical framework to assess the validity of vaccine allocation strategy in case of epidemic.

For COVID-19, the vaccination interval between the first and second doses was set as 3-4 weeks in many countries including the US. In the UK, this interval was set as 12 weeks in order to distribute the first doses to many people quickly [4]. Some papers constructed mathematical models to study how the vaccination interval affects the epidemic size [5,6]. In [5], it was shown that the relative efficacy (RE) of the first dose to the second one plays an important role in determining the optimal interval to minimize the total number of deaths. In [6], it was shown that the 12-week interval was highly beneficial to prevent the disease. A clinical study [7] showed that extending the vaccination interval from 3 weeks to 11-12 weeks boosts the peak antibody response by 3.5-fold in elderly people. In this paper, we propose a new age-structured mathematical model to investigate the optimal interval to minimize the total number of cases, deaths and deaths weighted by the average life expectancy. By using this model, we will show that the long interval as adopted in the UK can be justified if the RE is sufficiently high.

The ratio of vaccine allocation among different age groups is also important because the symptom and mortality of the disease and the pattern of social interactions during the epidemic highly depend on the individual's age. Thus, some previous studies have focused on this topic [8-12]. For COVID-19, prioritizing elderly people seems optimal because the mortality of COVID-19 is much higher in elderly people [9]. However, prioritizing young people also seems optimal because they tend to spread the infection to many people [10]. Some other studies focused on optimal allocation among not only age

groups but also geographical regions [11] and occupations [12]. In this paper, our model will be applied to investigate the optimal ratio of allocation among young and elderly people. We will show that, to reduce the number of deaths as well as the number of deaths weighted by the average life expectancy, prioritizing young people is optimal if the heterogeneity in the age-dependent susceptibility (HS) is high, whereas prioritizing elderly people is optimal if the HS is low. In addition, we will show that the heterogeneity in the contact frequency among different age classes (HC) affects the effectiveness of the vaccination campaign, for fixed basic reproduction number [13].

The organization of this paper is as follows: in section 2, we give an outline of our mathematical model (see Supplementary for details). We formulate an age-structured susceptible-exposed-infectious-recovered (SEIR) model with severe population (W). The vaccine efficacy is considered by introducing the class age structure into the vaccinated populations. In section 3, we investigate the optimal vaccination interval between the first and second doses. In section 4, we investigate the optimal vaccine allocation between young and elderly age groups. In section 5, we perform a counterfactual simulation that shows how the total number of COVID-19-related deaths in Japan from May 15, 2021 to November 30, 2021 could have been reduced if the optimal vaccine strategy had been taken. Finally, sections 6 and 7 are devoted to the discussion and conclusions, respectively.

2. Outline of the model

Let S, E, I, R and W denote the susceptible, exposed, infectious, recovered and severe populations, respectively. Let h and v be subscripts representing the vaccine hesitant and vaccinated, respectively. Let t, a and τ denote the time, chronological age and vaccine age (time elapsed since the first vaccination shot), respectively. For example, $S_v(t, a, \tau)$ represents the susceptible population of age a at time t with vaccine age τ, and $I_h(t, a)$ represents the infectious population with vaccine hesitancy of age a at time t. The transfer diagram of our model is shown in Figure 1.

For the full details of our model, see Supplementary. In our model, the units of time and vaccine age are set as 1 day, and the unit of age is set as 1 year. All independent variables t, a and τ are continuous and take values in $[0, t_{max}]$, $[0, a_{max}]$ and $[0, \tau_{max}]$, respectively. We assume $t_{max} = \tau_{max} = 232$ so that $t = 0$ corresponds to April 12, 2021, which is the day when the vaccination program for COVID-19 started in Japan, and $t = 232$ corresponds to November 30, 2021, which is the last day when only the first and second doses are distributed in Japan[5]. We assume $a_{max} = 100$. To run the

[5] Of course, by changing parameters, our model can be applied to other cases not restricted to

simulation program, we use the standard Euler forward method (see Figure S10 in Supplementary for the main part of our MATLAB code).

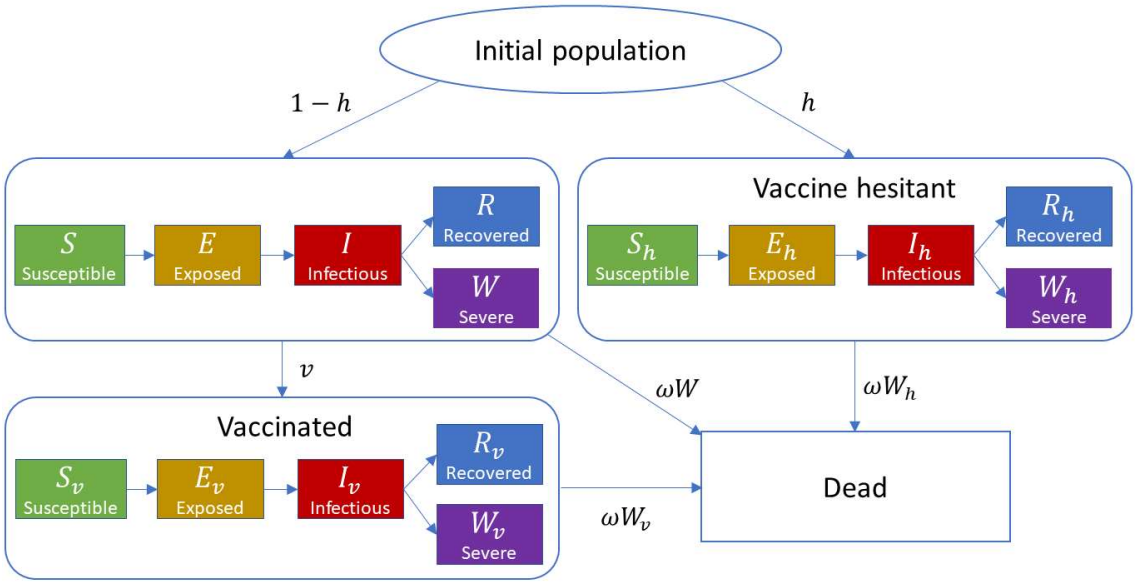

Figure 1. Transfer diagram of our model.

The force of infection in our model is given by

$$\lambda(t,a) = \int_0^{a_{max}} \beta(a,b)\left[I(t,b) + I_h(t,b) + \int_0^{\tau_{max}} I_v(t,b,\tau)d\tau\right]db,$$

where $\beta(a,b)$ denotes the transmission function between susceptible individuals aged a and infectious individuals aged b. We assume that $\beta(a,b)$ is expressed as

$$\beta(a,b) = \kappa\beta_1(a)\beta_2(a-b),$$

where κ is a scaling parameter adjusted to attain a fixed basic reproduction number $\mathcal{R}_0$ for different β_1 and β_2. $\beta_1 = \beta_1(a)$ is the susceptibility of those aged a, and $\beta_2 = \beta_2(x)$ is the contact frequency among individuals whose age difference is x. The HS is quantified by β_1 as shown in Figure 2 (left). We assume that β_1 is higher for young people than for elderly people aged over 65. We adopt this assumption because elderly

Japan.

people may be more likely to behave carefully and reduce their contact opportunities, taking into account the fact that the mortality of COVID-19 is higher for elderly people than for young people. The HC is quantified by β_2 as shown in Figure 2 (right). We assume that $\beta_2(x)$ has five peaks at $x = 0, \pm 30, \pm 60$. This assumpriotn means that the contact frequency across (i) children, (ii) their parents, and (iii) grandparents is higher than for other pairs. For the exact definition of β_1 and β_2, see Supplementary.

We consider three parameter configurations regarding β_1 and β_2. They are shown in three lines in each panel of Figure 2. The relative value of β_1 for young people (to that for elderly people) is larger in the "high HS" case than in the "low HS" case. People become more likely to contact to those with similar age—that is, the mixing becomes more heterogeneous—in the "high HC" case than in the "low HC" case.

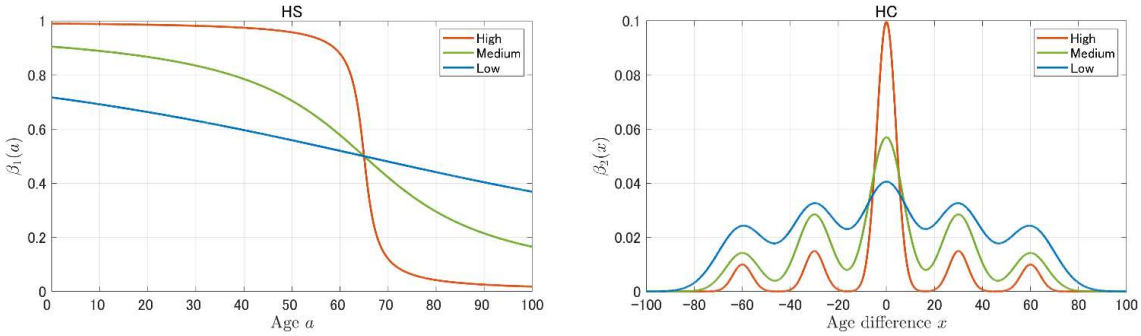

Figure 2. Age dependent susceptibility $\beta_1(a)$ (HS) and contact frequency $\beta_2(x)$ among individuals whose age difference is x (HC). For panel, the three levels of heterogeneity (high, medium and low) are considered.

The vaccine efficacies to reduce the infection and mortality risks are represented by $\sigma(\tau) \in [0,1]$ and $\delta(\tau) \in [0,1]$, respectively. They are assumed to be functions of vaccine age τ, and reduce the force of infection $\lambda(t,a)$ and the ratio $d(a)$ of which an infected individual becomes severe to $[1-\sigma(\tau)]\lambda(t,a)$ and $[1-\delta(\tau)]d(a)$, respectively. Specifically, they are defined as follows:

$$\sigma(\tau) = \begin{cases} 0, & 0 \le \tau < 14, \\ \sigma_1[1-k(\tau-14)], & 14 \le \tau < T, \\ \sigma_2[1-k(\tau-T)], & \tau \ge T, \end{cases} \quad \delta(\tau) = \begin{cases} 0, & 0 \le \tau < 14, \\ \delta_1[1-k(\tau-14)], & 14 \le \tau < T, \\ \delta_2[1-k(\tau-T)], & \tau \ge T, \end{cases}$$

where σ_i and δ_i $(i = 1,2)$ denote the efficacies of the i-th vaccination to reduce the infection and mortality risks, respectively. k denotes the waning rate of vaccine-induced immunity, and T denotes the length of the vaccination interval between the

first and second doses. k is fixed as $1/600$ so that the efficacies decrease to their half after about 300 days passed [14]. σ_i, δ_i $(i = 1,2)$ and T are varied in the subsequent sections to discuss the optimal strategy.

The per capita rate of vaccination in our model is defined by $v = v(t,a) = v_1(t)v_2(a)$, where $v_1(t)$ is a value estimated by using the vaccination data in Japan [15]. $v_2(a)$ is a function defined by

$$v_2(a) = \begin{cases} 0, & 0 \le a < 18, \\ 1-u, & 18 \le a < 65, \\ u, & a \ge 65, \end{cases}$$

where u is the proportion of vaccine allocation to those aged over 65. Thus, a higher u means prioritizing the elderly people. In the subsequent sections, u is also varied to investigate the optimal allocation ratio.

3. Optimal interval between the first and second vaccination doses

In this section, varying the vaccination interval between the first and second doses from 3 weeks $(T = 21)$ to 12 weeks $(T = 84)$, we investigate the optimal interval that minimizes the total number of cases, deaths and deaths weighted by the average life expectancy. We assume that the basic reproduction number is fixed as $\mathcal{R}_0 = 1.5$, a sensible number for a disease like pandemic influenza [16] and set both of the HS and HC to medium (see Figure 2). In reality, the contact matrix evolved over time reflecting changes in policies and behaviors, but we abstract from such time-variation in our analysis. We compare two cases where the allocation ratio is $u = 0.1$ (prioritizing young people) and $u = 0.9$ (prioritizing elderly people). To consider the relative efficacy (RE) of the first dose to the second one, we assume that $\sigma_2 = \delta_2 = 1$, and compare three cases where $\sigma_1 = \delta_1 = 0.2$ (RE $= 0.2$); 0.5 (RE $= 0.5$); 0.8 (RE $= 0.8$).

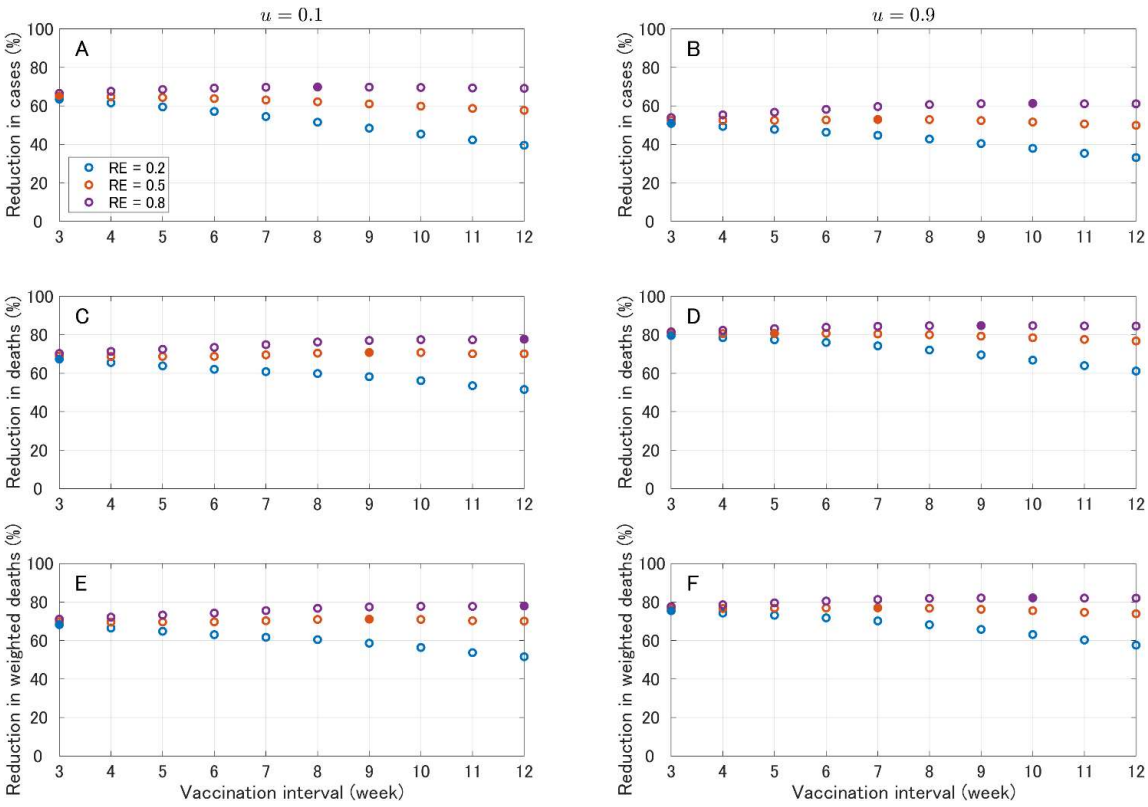

Figure 3. Reduction ratio in cases (A and B), deaths (C and D) and deaths weighted by the average life expectancy (E and F) versus the vaccination interval between the first and second doses. Proportion of vaccine allocation to the elderly people is 0.1 in A, C and E, and is 0.9 in B, D and F. RE implies the relative efficacy of the first dose compared to the second one. The filled circles represent that they are optimal.

Figure 3 shows that the RE plays the central role in determining the optimal interval. In Figure 3, irrespective of the allocation ratio u, the optimal intervals for all objectives (cases, deaths and deaths weighted by the average life expectancy) tend to become long as the RE increases. We can interpret this as follows: if the RE is low, then the first dose is less effective, and thus, prioritizing the rollout of the second doses by shortening the interval is optimal; if the RE is high, then the first dose is sufficiently effective, and thus, prioritizing the rollout of the first doses by enlarging the interval is optimal.

We next consider a more special case where the vaccine efficacies are selected for vaccines of Pfizer and AstraZeneca. By taking the mean of the data in [17], we set

$$(\sigma_1, \sigma_2, \delta_1, \delta_2) = \begin{cases} (0.63, 0.90, 0.80, 0.94), & \text{Pfizer}, \\ (0.62, 0.64, 0.80, 0.85), & \text{AstraZeneca}. \end{cases} \tag{1}$$

In both of these two cases, the long interval is optimal to maximize the reduction ratio of all objectives (see Figure 4). This result suggests that the 12-week interval taken in the UK was reasonable. In addition, we can see from Figure 4 that the optimal intervals for Pfizer are shorter than those for AstraZeneca, reflecting the fact that the RE of AstraZeneca is higher than that of Pfizer.

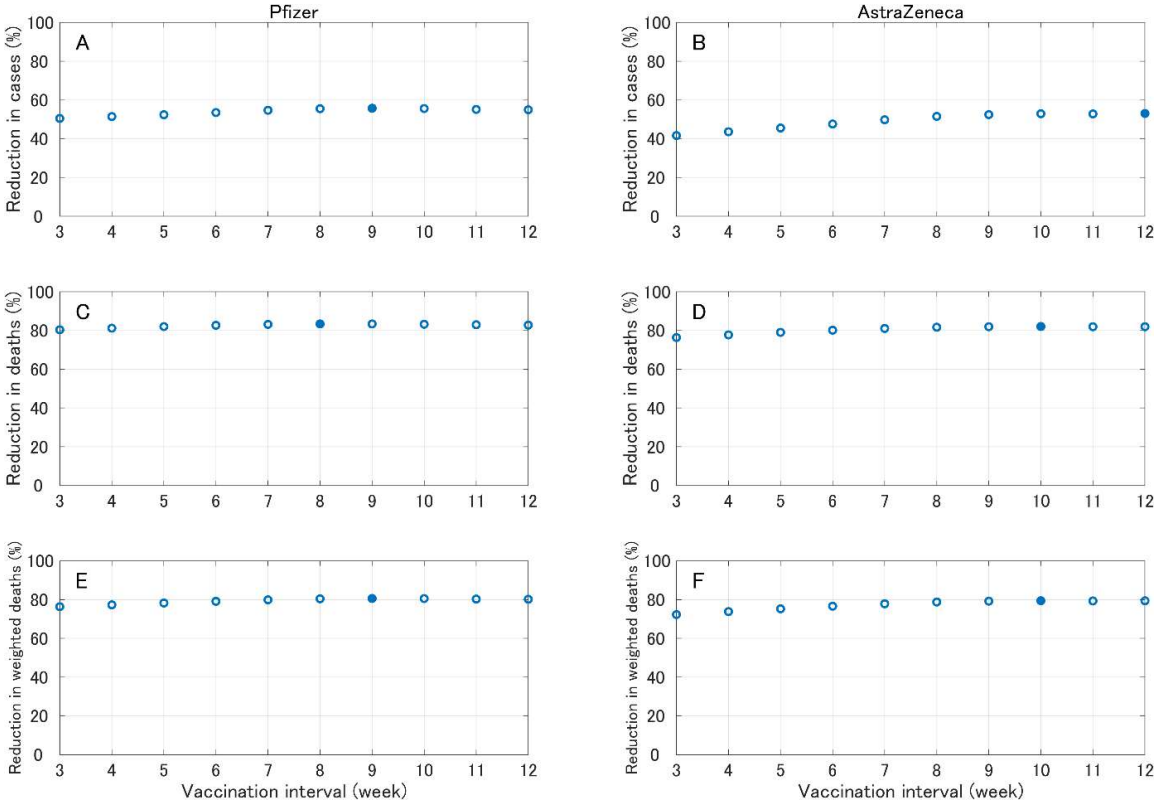

Figure 4. Reduction ratio in cases (A and B), deaths (C and D) and deaths weighted by the average life expectancy (E and F) versus the vaccination interval between the first and second doses (A, C and E: Pfizer; B, D and F: AstraZeneca). The filled circles represent that they are optimal.

4. Optimal ratio of allocation among young and elderly people

In this section, varying the ratio u of vaccine allocation to the elderly people from 0.1 to 0.9, we investigate the optimal ratio that minimizes the total number of cases, deaths and deaths weighted by the average life expectancy. We fix the basic reproduction number as $\mathcal{R}_0 = 1.5$, as in the previous section, and the vaccination interval between the first and second doses as 3 weeks. The vaccine efficacy is chosen as for Pfizer in Eq. (1). We vary the HS and the HC (see Figure 2), and investigate how they affect the optimal allocation

ratio.

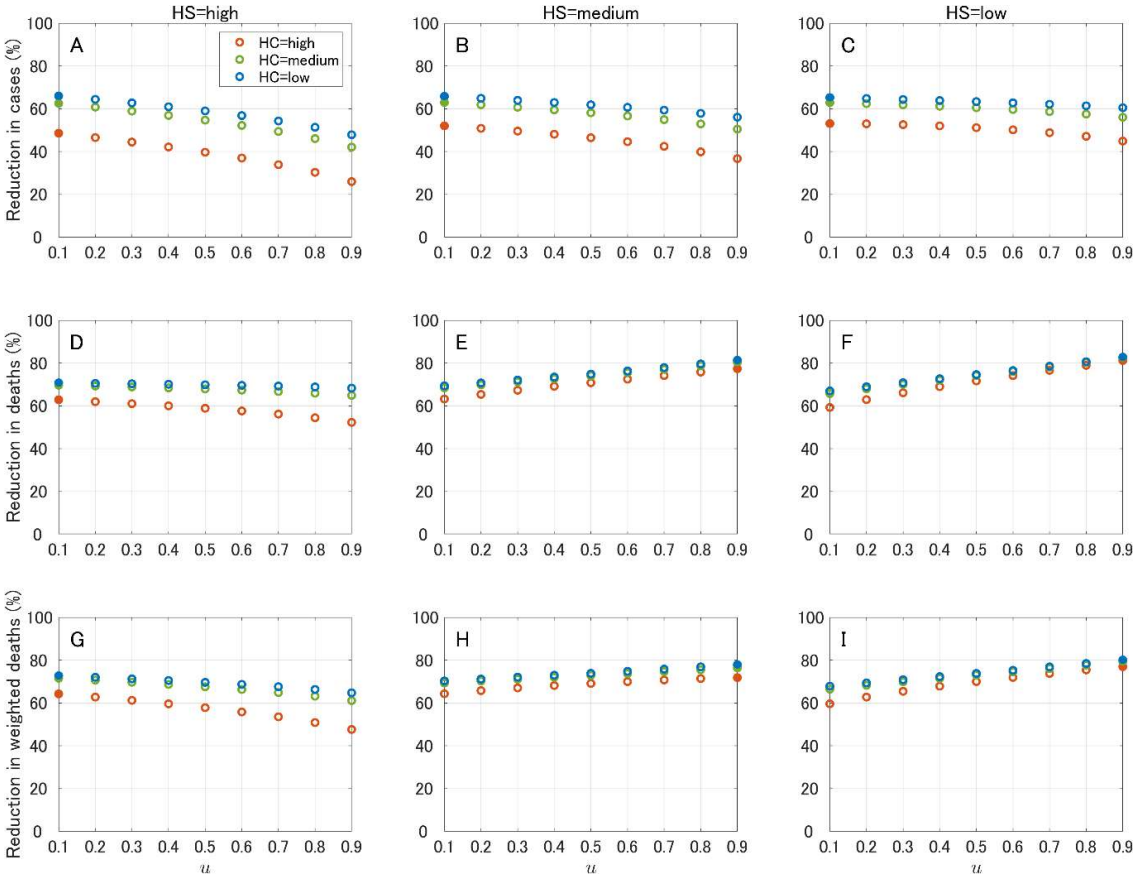

Figure 5. Reduction ratio in cases (A-C), deaths (D-F) and deaths weighted by the average life expectancy (G-I) versus the ratio of vaccine allocation to the elderly people (u). The filled circles represent that they are optimal.

From Figure 5, A-C and Table 1, we see that, to reduce the total number of cases, prioritizing young people $(u = 0.1)$ is always optimal. On the other hand, from Figure 5, D-I and Table 1, we see that the optimal ratio to maximize the reduction ratio of deaths and deaths weighted by the average life expectancy is more sensitive to the HS: if HS is high, then prioritizing young people $(u = 0.1)$ is optimal, whereas if HS is medium or low, then prioritizing elderly people $(u = 0.9)$ is optimal. This seems natural because if young people are more likely to be infected (the HS is high), then prioritizing them becomes optimal to stop the disease spread. If the HS is low, then prioritizing elderly people is optimal because they have high mortality for COVID-19. In addition, from Figure 5 and Table 1, we can see that the HC does not affect the optimal allocation ratio in all cases. However, the effectiveness of the vaccination is reduced as the HC increases.

From this result, we can conjecture that the vaccination program is more effective in a population well-mixed among different age groups. Here, note that the basic reproduction number $\mathcal{R}_0$ is fixed and just the contact frequency is changed in our simulation (see Supplementary for how to fix $\mathcal{R}_0$).

Table 1. A summary on the results in Figure 5.

Object	**(HS, HC)**	u **in optimal**	**reduction ratio in optimal (%)**
cases	(high, high)	0.1 (young)	48.63
cases	(high, medium)	0.1 (young)	62.58
cases	(high, low)	0.1 (young)	66.02
cases	(medium, high)	0.1 (young)	52.04
cases	(medium, medium)	0.1 (young)	62.99
cases	(medium, low)	0.1 (young)	65.84
cases	(low, high)	0.1 (young)	53.12
cases	(low, medium)	0.1 (young)	62.92
cases	(low, low)	0.1 (young)	65.26
deaths	(high, high)	0.1 (young)	62.89
deaths	(high, medium)	0.1 (young)	69.67
deaths	(high, low)	0.1 (young)	70.76
deaths	(medium, high)	0.9 (elderly)	77.39
deaths	(medium, medium)	0.9 (elderly)	80.36
deaths	(medium, low)	0.9 (elderly)	81.33
deaths	(low, high)	0.9 (elderly)	81.21
deaths	(low, medium)	0.9 (elderly)	82.38
deaths	(low, low)	0.9 (elderly)	82.77
weighted deaths	(high, high)	0.1 (young)	64.25
weighted deaths	(high, medium)	0.1 (young)	71.56
weighted deaths	(high, low)	0.1 (young)	72.72
weighted deaths	(medium, high)	0.9 (elderly)	71.87
weighted deaths	(medium, medium)	0.9 (elderly)	76.37
weighted deaths	(medium, low)	0.9 (elderly)	77.90
weighted deaths	(low, high)	0.9 (elderly)	76.98
weighted deaths	(low, medium)	0.9 (elderly)	79.23
weighted deaths	(low, low)	0.9 (elderly)	80.08

5. Counterfactual simulation

In this section, fitting our model to the real data of reported cases in Japan from April 12, 2021 to November 30, 2021 [18], we estimate the time-varying transmission rate. Specifically, we compute the transmission rate on each day that minimizes the sum of the squares error between the real data of the newly reported cases in past 7 days and its simulation counterparts. To our knowledge, no previous study has used a similar method. In the estimation, we made the following assumptions (see Supplementary for more details):

- The HS and the HC are medium;
- The vaccination interval is 3 weeks;
- The vaccine allocation ratio is $u = 0.9$ (prioritizing elderly people);
- The detection ratio (the ratio at which a newly infected individual is finally reported) is 0.5.

We then change the vaccination interval and the allocation ratio, and investigate how the total number of deaths could be reduced in the optimal case. The curve fitted to the daily number of newly reported deaths is shown in Figure 6, bottom (see the red curve). In this case, the total number of deaths is 8,793. On the other hand, our simulation shows that the total number of deaths is minimized when the vaccination interval is 9 weeks and the allocation ratio is $u = 0.9$ (see Figure 6, top). If such an optimal strategy is taken, then the total number of deaths is reduced to 7,176. In particular, the blue curve in the bottom panel of Figure 6 suggests that the epidemic wave of August 2021 could have been avoided if the optimal strategy had been taken.

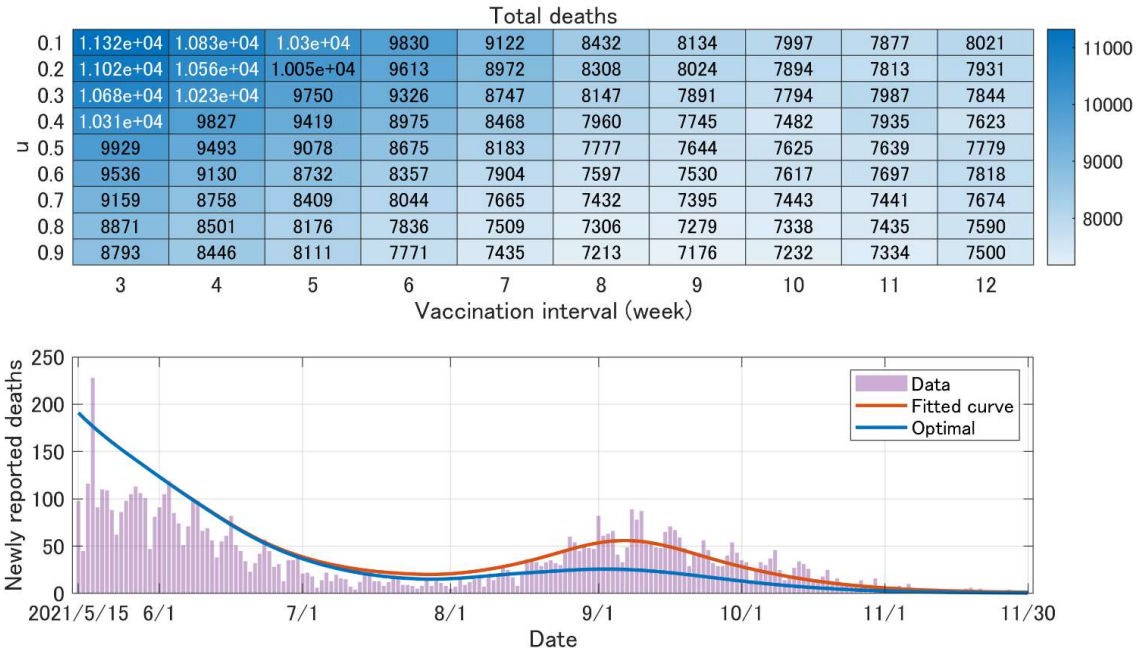

Figure 6. (Top) Total number of disease-induced deaths for different vaccination interval and allocation ratio u; (Bottom) Daily number of newly reported deaths with the fitted curve (red) and the curve for the optimal case (blue).

6. Discussion

In this paper, we have proposed an age-structured epidemic model and investigated the optimal vaccination interval between the first and second doses, and the optimal vaccine allocation among young and elderly people. Although we used the data of COVID-19 in Japan in this paper, our model can be applied to various infectious diseases in countries not limited to Japan. The methodology constructed in this paper would help us to design an appropriate vaccine rollout program promptly in case of a future pandemic.

Our result on the optimal interval between the first and second doses has indicated that the RE plays the central role in determining the optimal interval: the short interval is optimal if the RE is low, whereas the long interval is optimal if the RE is high. This result is in line with the previous result in [5] that a longer interval can be optimal to minimize the number of deaths if the first dose presents a higher level of relative efficacy in the case of limited vaccine supply.

Moreover, for both cases of the Pfizer and AstraZeneca vaccines, our simulation has suggested that the optimal interval is longer or equal to 8 weeks. More precisely, 8-9 weeks interval can be optimal for the Pfizer vaccine and 10-12 weeks interval can be optimal for the AstraZeneca vaccine to reduce the number of cases, deaths as well as the

number of deaths weighted by the average life expectancy. This result is in line with the previous result in [6] for the data in UK that the 12-week interval can be highly beneficial to reduce the number of hospital admissions and deaths. Hence, the 12-week interval taken in the UK for COVID-19 seems sensible. In case of a future pandemic, it is important to know accurate information on the vaccine efficacy to design efficient vaccine allocation strategies. If the amount of available vaccines is limited and the efficacy of the first dose is not low, then it would be worth considering about prolonging the vaccination interval.

Our result on the vaccine allocation among young and elderly people has shown that the optimal allocation ratio to minimize the number of deaths as well as the number of deaths weighted by the average life expectancy depends importantly on the HS. Prioritizing young people can be justified if the HS is high, that is, young people are more likely to be infected as they tend to go out more. In [10], it was shown that prioritizing high-transmission (younger) age groups can minimize the number of deaths if the vaccine efficacy is higher than 60%. Our result is consistent with the previous result in [10] because the vaccine efficacy in our simulation is higher than 60% (see Eq. (1)). Our result has also shown that the effectiveness of the vaccination campaign increases as the HC decreases. This result has suggested that the vaccination program can be more effective in a population well-mixed among different age groups.

Our counterfactual simulation has suggested that the epidemic wave in the summer of 2021 in Japan could have been avoided if the optimal vaccine strategy had been taken. In our simulation, we assumed that the HS and HC are medium and the detection ratio is 0.5. Comparing the number of deaths in simulation for different vaccination intervals and allocation ratios, our optimal strategy to minimize the number of deaths recommended the 9-week interval and prioritizing elderly people ($u = 0.9$).

We end our discussion by pointing out several limitations of our study.

First, as in any simulation studies, the optimal strategy would depend on the assumed parameter values. For example, the amount of available vaccines would affect the optimal interval because if there are many vaccines so that all people can get vaccinated twice soon, then shortening the interval to prioritize the second shot would be optimal.

Second, we focus on the optimal allocation in a short time period (232 days from April 12, 2021 to November 30, 2021 in Japan) for the sake of simplicity. An extended optimization in a longer time period could be useful in designing suitable vaccination strategy, even though we might have to take into account the effect of booster shots and simulation might have to become more complex.

Third, we abstracted from how the vaccination interval affects the immune response. However, as a clinical study [7] suggested, a long interval could help in increasing the peak of the antibody response. Thus, the long vaccination interval could be justified from not only mathematical but also clinical points of view.

Fourth, we estimated the infection rate in our counterfactual simulation for Japan, 2021 using data from a fixed past period. If we had taken an alternative vaccination strategy and the number of reported cases and deaths had changed as a result, people's behavior could have also changed. In general, our assumption that the detection rate of infection was fixed over time is a useful starting point for analysis, but the infection rate can change according to policies, social norms, seasonality, and virus mutation.

7. Conclusion

We have constructed an age-structured epidemic model to evaluate the vaccination interval between the first and second doses and the vaccine allocation strategy between young and elderly age groups. The RE plays an important role in determining the optimal vaccination interval. The optimal interval tends to become longer as the RE increases. The HS tends to affect the optimal allocation between young and elderly people. On the other hand, the HC tends to affect the effectiveness of the vaccination campaign. The counterfactual simulation for COVID-19 in Japan in 2021 has indicated that the epidemic wave in the summer of 2021 in Japan could have been avoided if the optimal vaccine allocation strategy had been taken.

References

1. S. Flaxman, S. Mishra, A. Gandy, H.J.T. Unwin, T.A. Mellan, H. Coupland, et al., Estimating the effects of non-pharmaceutical interventions on COVID-19 in Europe, *Nature*, **584** (2020), 257-261. https://doi.org/10.1038/s41586-020-2405-7
2. M. Nicola, Z. Alsafi, C. Sohrabi, A. Kerwan, A. Al-Jabir, C. Iosifidis, et al., The socio-economic implications of the coronavirus pandemic (COVID-19): A review, *International Journal of Surgery*, **78** (2020), 185-193. https://doi.org/10.1016%2Fj.ijsu.2020.04.018
3. *World Health Organization*, WHO SAGE Roadmap for prioritizing uses of COVID-19 vaccines in the context of limited supply, 2020.

Available from: https://www.who.int/docs/default-source/immunization/sage/covid/sage-prioritization-roadmap-covid19-vaccines.pdf

4. *Joint Committee on Vaccination and Immunisation*, Prioritising the first COVID-19 vaccine dose: JCVI statement, 2021. Available from: https://www.gov.uk/government/publications/prioritising-the-first-covid-19-vaccine-dose-jcvi-statement
5. L.S. Ferreira, O. Canton, R.L.P. Silva, S. Poloni, V. Sudbrack, M.E. Borges, et al., Assessing the best time interval between doses in a two-dose vaccination regimen to reduce the number of deaths in an ongoing epidemic of SARS-CoV-2, *PLoS Computational Biology*, **18** (2022), e10009978. https://doi.org/10.1371/journal.pcbi.1009978
6. M.J. Keeling, S. Moore, B.S. Penman, E.M. Hill, The impacts of SARS-CoV-2 vaccine dose separation and targeting on the COVID-19 epidemic in England, *Nature Communications*, **14** (2023), 740. https://doi.org/10.1038/s41467-023-35943-0
7. H. Parry, R. Bruton, C. Stephens, C. Bentley, K. Brown, G. Amirthalingam, et al., Extended interval BNT162b2 vaccination enhances peak antibody generation, *NPJ Vaccines*, **7** (2022), 14. https://doi.org/10.1038/s41541-022-00432-w
8. K.M. Bubar, K. Reinholt, S.M. Kissler, M. Lipsitch, S. Cobey, Y.H. Grad, et al., Model-informed COVID-19 vaccine prioritization strategies by age and serostatus, *Science*, **371** (2021), 916-921. https://doi.org/10.1126/science.abe6959
9. B.H. Foy, B. Wahl, K. Mehta, A. Shet, G.I. Menon, C. Britto, Comparing COVID-19 vaccine allocation strategies in India: a mathematical modelling study, *International Journal of Infectious Diseases*, **103** (2021), 431-438. https://doi.org/10.1016/j.ijid.2020.12.075
10. L. Matrajt, J. Eaton, T. Leung, E.R. Brown, Vaccine optimization for COVID-19: who to vaccinate first?, *Science Advances*, **7** (2021), eabf1374. https://doi.org/10.1126/sciadv.abf1374
11. J. Molla, A.P.L. Chávez, T. Hiraoka, T. Ala-Nissila, M. Kivelä, L. Leskelä, Adaptive and optimized COVID-19 vaccination strategies across geographical regions and age groups, *PLoS Comput. Biol.*, **18** (2022), e1009974. https://doi.org/10.1371/journal.pcbi.1009974
12. A. Babus, S. Das, S. Lee, The optimal allocation of COVID-19 vaccines, *Economics Letters*, **224** (2023) 111008. https://doi.org/10.1016/j.econlet.2023.111008

13. O. Diekmann, J.A.P. Heesterbeek, J.A.J. Metz, On the definition and the computation of the basic reproduction ratio R0 in models for infectious diseases in heterogeneous populations, *Journal of Mathematical Biology*, **28** (1990), 365–382. https://doi.org/10.1007/BF00178324
14. S. Kodera, E.A. Rashed, A. Hirata, Estimation of Real-World Vaccination Effectiveness of mRNA COVID-19 Vaccines against Delta and Omicron Variants in Japan, *Vaccines*, **10** (2022), 430. https://doi.org/10.3390/vaccines10030430
15. *Digital Agency*, Vaccination Record System (VRS).
Available from: https://info.vrs.digital.go.jp/opendata/ (Japanese)
16. C. Fraser, C.A. Donnelly, S. Cauchemez, W.P. Hanage, M.D. Kerkhove, T.D. Hollingsworth, et al., Pandemic potential of a strain of influenza A (H1N1): early findings, *Science*, **324** (2009) 1557-1561. https://doi.org/10.1126/science.1176062
17. *SPI-M-O*, Summary of further modelling of easing restrictions – Roadmap Step 2 (2021).
Available from:
https://assets.publishing.service.gov.uk/government/uploads/system/uploads/attachment_data/file/975909/S1182_SPI-M-O_Summary_of_modelling_of_easing_roadmap_step_2_restrictions.pdf
18. *Ministry of Health, Labour and Welfare of Japan*, Visualizing the data: information on COVID-19 infections.
Available from: https://covid19.mhlw.go.jp/en/

Supplementary Materials

for

"Optimal Vaccine Allocation Strategy: Theory and Application to the Early Stage of COVID-19 in Japan"

Mathematical model

The main model in this study is the following PDEs system (see Figure S1)[6]:

$$\partial_t S = -\lambda(t,a)S - v(t,a)S,$$
$$\partial_t E = \lambda(t,a)S - \varepsilon E - v(t,a)E,$$
$$\partial_t I = \varepsilon E - \gamma I - v(t,a)I,$$
$$\partial_t R = [1-d(a)]\gamma I - v(t,a)R,$$
$$\partial_t W = d(a)\gamma I - \omega W,$$

$$\partial_t S_h = -\lambda(t,a)S_h,$$
$$\partial_t E_h = \lambda(t,a)S_h - \varepsilon E_h,$$
$$\partial_t I_h = \varepsilon E_h - \gamma I_h,$$
$$\partial_t R_h = [1-d(a)]\gamma I_h,$$
$$\partial_t W_h = d(a)\gamma I_h - \omega W_h,$$

$$(\partial_t + \partial_\tau)S_v = -[1-\sigma(\tau)]\lambda(t,a)S_v,$$
$$(\partial_t + \partial_\tau)E_v = [1-\sigma(\tau)]\lambda(t,a)S_v - \varepsilon E_v,$$
$$(\partial_t + \partial_\tau)I_v = \varepsilon E_v - \gamma I_v,$$
$$(\partial_t + \partial_\tau)R_v = \{1-[1-\delta(\tau)]d(a)\}\gamma I_v,$$
$$\partial_t W_v = \int_0^{\tau_{max}} [1-\delta(\tau)]d(a)\gamma I_v d\tau - \omega W_v,$$

$$S_v(t,a,0) = v(t,a)S(t,a),\ E_v(t,a,0) = v(t,a)E(t,a),$$
$$I_v(t,a,0) = v(t,a)I(t,a),\ R_v(t,a,0) = v(t,a)R(t,a),$$

[6] We disregard the aging process assuming $\partial_a S = 0,\ \partial_a E = 0$, …, etc., because the time span of our simulation is less than 1 year.

$$S(0,a) = [1-h(a)]S_0(a),\ E(0,a) = [1-h(a)]E_0(a),$$
$$I(0,a) = [1-h(a)]I_0(a),\ R(0,a) = [1-h(a)]R_0(a),\ W(0,a) = [1-h(a)]W_0(a),$$
$$S_h(0,a) = h(a)S_0(a),\ E_h(0,a) = h(a)E_0(a),\ I_h(0,a) = h(a)I_0(a),\ R_h(0,a) = h(a)R_0(a),$$
$$W_h(0,a) = h(a)W_0(a),\ S_v(0,a,0) = E_v(0,a,0) = I_v(0,a,0) = R_v(0,a,0) = W_v(0,a) = 0,$$

$$\lambda(t,a) = \int_0^{a_{max}} \beta(a,b)\left[I(t,b) + I_h(t,b) + \int_0^{\tau_{max}} I_v(t,b,\tau)d\tau\right]db.$$

The description of each symbol is as follows (see also Table S1):

- $t\ (0 \le t \le t_{max})$: time;
- $a\ (0 \le a \le a_{max})$: age;
- $\tau\ (0 \le \tau \le \tau_{max})$: vaccine age (time elapsed since the first vaccination);
- $S = S(t,a)$: susceptible population;
- $S_h = S_h(t,a)$: vaccinated susceptible population;
- $S_v = S_v(t,a,\tau)$: susceptible population who have been vaccinated;
- $E = E(t,a)$: exposed (pre-infectious) population;
- $E_h = E_h(t,a)$: exposed population with vaccine hesitancy;
- $E_v = E_v(t,a,\tau)$: vaccinated exposed population;
- $I = I(t,a)$: infectious (with and without symptoms) population;
- $I_h = I_h(t,a)$: infectious population with vaccine hesitancy;
- $I_v = I_v(t,a,\tau)$: vaccinated infectious population;
- $R = R(t,a)$: recovered population;
- $R_h = R_h(t,a)$: recovered population with vaccine hesitancy;
- $R_v = R_v(t,a,\tau)$: vaccinated recovered population;
- $W = W(t,a)$: severe population;
- $W_h = W_h(t,a)$: severe population with vaccine hesitancy;
- $W_v = W_v(t,a)$: vaccinated severe population;
- $\lambda(t,a)$: force of infection;
- $v(t,a)$: vaccination rate;
- ε: transition rate from the exposed class to the infectious class;
- γ: removal rate;
- $d(a)$: ratio at which an infected individual enters the severe class;
- ω: mortality rate of severe individuals;
- $\sigma(\tau)$: vaccine efficacy to reduce the infection risk;
- $\delta(\tau)$: vaccine efficacy to reduce the mortality risk;
- $h(a)$: vaccine hesitancy rate;

- $\beta(a,b)$: transmission function between susceptible individuals of age a and infectious individuals of age b.

Parameter setting

The unit time is set as 1 day. In Japan, the COVID-19 vaccination program for ordinary people started at April 12, 2021, and the booster (third) vaccination started at December 1, 2021. Because, in this study, we focus on the optimal interval between the first and second doses, we set the time range in our simulation from April 12, 2021 ($t = 0$) to November 30, 2021 ($t = t_{max} = 232$). As the vaccine age does not exceed the calendar time, we set $\tau_{max} = 232$. Let the unit age be 1 year, and the age interval be $[0,100]$, that is, $a_{max} = 100$.

We set $\varepsilon = 0.2$ and $\gamma = 0.1$ so that the average incubation period is $1/\varepsilon = 5$ days [1,2] and the average infectious period is $1/\gamma = 10$ days [3]. We assume that the severe class is composed of individuals who will die due to COVID-19, and set $d(a)$ as shown in Figure S2 by dividing the cumulative deaths by the cumulative cases in each age class as of November 30, 2021, using the open data in [4]. The vaccine hesitancy rate $h(a)$ is estimated as in Figure S3 using the vaccination data in [5].

For the initial condition, let

$$P_0(a) = S_0(a) + E_0(a) + I_0(a) + R_0(a) + W_0(a),$$

be the population age distribution in Japan as of April 2021 ($t = 0$). Using the data in [6], we fix $P_0(a)$ as shown in Figure S4. Here, we normalize $P_0(a)$ so that $\int_0^{a_{max}} P_0(a)da = 1$. Each population then describes a proportion to the total population. For simplicity, we assume that $W_0(a) = 0$, and fix $E_0(a), I_0(a)$ and $R_0(a)$ as shown in Figure S5 using the data in [4]. $S_0(a)$ can then be calculated as $P_0(a) - E_0(a) - I_0(a) - R_0(a)$.

We assume that the infection rate $\beta(a,b)$ has the following form:

$$\beta(a,b) = \kappa\beta_1(a)\beta_2(a-b),$$

where κ is the infection transmission rate, $\beta_1(a)$ is the age-dependent susceptibility, and $\beta_2(x)$ is a distance function representing the contact frequency among individuals whose age difference is x. More precisely, according to the three levels of heterogeneity (high, medium and low), we set $\beta_1(a)$ and $\beta_2(x)$ as follows (see Figure S6):

$$\beta_1(a) = \begin{cases} \mathrm{Arctan}(-(a-65)/2)/\pi + 1/2, & \text{high,} \\ \mathrm{Arctan}(-(a-65)/20)/\pi + 1/2, & \text{medium,} \\ \mathrm{Arctan}(-(a-65)/80)/\pi + 1/2, & \text{low,} \end{cases}$$

$$\beta_2(x) = \begin{cases} f_{0,4}(x) + 0.15\left(f_{30,4}(x) + f_{-3\ ,4}(x)\right) + 0.1\left(f_{60,4}(x) + f_{-60,4}(x)\right), & \text{high,} \\ f_{0,7}(x) + 0.5\left(f_{30,7}(x) + f_{-30,7}(x)\right) + 0.25\left(f_{60,7}(x) + f_{-6\ ,7}(x)\right), & \text{medium,} \\ f_{0,10}(x) + 0.8\left(f_{30,10}(x) + f_{-3\ ,10}(x)\right) + 0.6\left(f_{60,10}(x) + f_{-6\ ,10}(x)\right), & \text{low,} \end{cases}$$

where $f_{\mu,\sigma}(x)$ denotes the probability density function of normal distribution with mean μ and standard derivation σ. $\beta_1(a)$ represents the heterogeneity in the age-dependent susceptibility (HS) and $\beta_2(x)$ represents the heterogeneity in the contact frequency among different age classes. The reason why we assume that $\beta_1(a)$ is higher in younger age group is that elderly people might be more careful and more likely to reduce the contact opportunity because the mortality of COVID-19 is quite high in those people. The reason why we assume that $\beta_2(x)$ has five peaks is that the contact opportunity among children and their parents and grandparents might be high. In addition, we assume that if $\beta_2(x)$ (HC) is high, then people become more likely to contact with people in similar age group, whereas if $\beta_2(x)$ (HC) is low, then people become more likely to contact beyond age groups and the mixing becomes more homogeneous. The parameter κ is modified to fix the basic reproduction number $\mathcal{R}_0$ for different $\beta_1(a)$ and $\beta_2(x)$. Following the classical theory [7], $\mathcal{R}_0$ is defined by the spectral radius $r(K)$ of the following next generation operator K:

$$K\varphi(a) = \kappa P_0(a)\int_0^{a_{max}} \beta_1(a)\beta_2(a-b)\int_0^b e^{-\int_\rho^b [\gamma + d(\eta)]d\eta}\varphi(\rho)\,d\rho db.$$

We can numerically compute $r(K)$ by using a discretization method as in [8]. If we consider the case of $\mathcal{R}_0 = 1.5$, then κ is modified so that $r(K) = 1.5$ is attained (note that $r(K)$ is proportional to κ).

Let T be the length of the vaccination interval between the first and second doses. Assuming that severe individuals would not be newly vaccinated, the number of the first vaccination shots at time t is calculated as

$$\int_0^{a_{max}} v(t,a)[S(t,a) + E(t,a) + I(t,a) + R(t,a)]da \times N,$$

where $N = 1.26 \times 10^8$ is the total population in Japan as of 2021 [6]. The number of the second vaccination shots at time t is given by

$$\int_0^{a_{max}} [S_v(t,a,T) + E_v(t,a,T) + I_v(t,a,T) + R_v(t,a,T)]da \times N.$$

We assume that the vaccination rate is separable:

$$(1) \quad v(t,a) = v_1(t)v_2(a).$$

It then follows that

$$v_1(t) = \frac{V(t)/N - \int_0^{a_{max}} [S_v(t,a,T) + E_v(t,a,T) + I_v(t,a,T) + R_v(t,a,T)]da}{\int_0^{a_{max}} v_2(a)[S(t,a) + E(t,a) + I(t,a) + R(t,a)]da},$$

where $V(t)$ denotes the total number of vaccination at time t. We fix $V(t)$ as shown in Figure S7 using the data of vaccine distribution for COVID-19 in Japan from April 12, 2021 to November 30, 2021 [5]. $v_2(a)$ can be used to incorporate the priority of vaccine allocation to individuals aged a. We assume that

$$v_2(a) = \begin{cases} 0, & 0 \le a < 18, \\ 1-u, & 18 \le a < 65, \\ u, & a \ge 65, \end{cases}$$

where $u \in [0.1,0.9]$ denotes the ratio of vaccine allocation to those aged over 65. The vaccine efficacy is set as

$$(2) \quad \sigma(\tau) = \begin{cases} 0, & 0 \le \tau < 14, \\ \sigma_1[1-k(\tau-14)], & 14 \le \tau < T, \\ \sigma_2[1-k(\tau-T)], & \tau \ge T, \end{cases} \quad \delta(\tau) = \begin{cases} 0, & 0 \le \tau < 14, \\ \delta_1[1-k(\tau-14)], & 14 \le \tau < T, \\ \delta_2[1-k(\tau-T)], & \tau \ge T, \end{cases}$$

where σ_i and δ_i $(i = 1,2)$ denote the efficacy of the i-th vaccination in reducing the risk of infection and the risk of disease-related death, respectively. Here, according to [9], we assume that the vaccine efficacy linearly decreases with waning rate $k > 0$. In this study, we fix $k = 1/600$ so that the efficacy decreases to its half after 300 days passed [9]. We consider the Pfizer and AstraZeneca vaccines taking the mean of a dataset in [10]:

$$(\sigma_1, \sigma_2, \delta_1, \delta_2) = \begin{cases} (0.63, 0.90, 0.80, 0.94), & \text{Pfizer}, \\ (0.62, 0.64, 0.80, 0.85), & \text{AstraZeneca}. \end{cases}$$

Objective functions

To evaluate the effectiveness of vaccination program, we calculate the total number of cases as

$$H_1 = \int_0^{t_{max}} \int_0^{a_{max}} \lambda(t,a) \left\{ S(t,a) + S_h(t,a) + \int_0^{\tau_{max}} [1-\sigma(\tau)] S_v(t,a,\tau) d\tau \right\} da\, dt \times N,$$

and the total number of disease-induced deaths as

$$H_2 = \omega \int_0^{t_{max}} \int_0^{a_{max}} [W(t,a) + W_h(t,a) + W_v(t,a)] da\, dt \times N.$$

Let $\ell(a)$ be the average life expectancy at age a, which is estimated from the data in [11] as shown in Figure S8. The total number of disease-induced deaths weighted by the average life expectancy is as follows:

$$H_3 = \omega \int_0^{t_{max}} \int_0^{a_{max}} \ell(a) [W(t,a) + W_h(t,a) + W_v(t,a)] da\, dt \times N.$$

To compute the reduction ratio, we divide each of these functions by those without vaccination ($V(t) = 0$).

Counterfactual simulation for Japan in 2021

For the baseline scenario, we assume that the vaccination interval between the first and second doses is 3 weeks, the vaccine efficacy is as of Pfizer, the ratio u of vaccine allocation to the elderly people is 0.9, and both β_1 and β_2 are medium. We then estimate the time-varying infection rate with $\kappa = \kappa(t)$ by fitting the following function to the daily reported cases in Japan:

$$Y(t) := \chi \int_0^{a_{max}} \lambda(t,a) \left\{ S(t,a) + S_h(t,a) + \int_0^{\tau_{max}} [1-\sigma(\tau)] S_v(t,a,\tau) d\tau \right\} da \times N,$$

where χ is the detection ratio, that is, the ratio at which a newly infected individual is finally reported. More precisely, to estimate the infection rate on a day, we compare the simulation result and the real data of the newly reported cases in past 7 days, and find the parameter that minimizes the sum of the squares error. In our simulation, we assume that $\chi = 0.5$. The comparison of the curve of $Y(t)$ and the real data [4] is shown in Figure S9, top. Note that this function $Y(t)$ is uniquely calculated. For this estimated infection rate, we compare the daily number of newly reported deaths

$$D(t) = \omega \int_0^{a_{max}} [W(t,a) + W_h(t,a) + W_v(t,a)]da \times N,$$

and the real data [4] as shown in Figure S9, bottom. Here, for a technical reason on the fitting of $D(t)$, we compare the total deaths in the period from May 15, 2021 to November 30, 2021. Regarding this setting as a baseline, we investigate how the total deaths could be reduced if the optimal vaccination interval and the optimal ratio of allocation to the elderly people had been taken.

Numerical scheme

To run the simulation program, we use the standard Euler forward method. See Figure S10 for the main part of the program code for MATLAB.

References

1. S.A. Lauer, K.H. Grantz, Q. Bi, F.K. Jones, Q. Zheng, H.R. Meredith, et al, The Incubation Period of Coronavirus Disease 2019 (COVID-19) From Publicly Reported Confirmed Cases: Estimation and Application, *Ann. Intern. Med.*, **172** (2020), 577-582. https://doi.org/10.7326/M20-0504
2. N.M. Linton, T. Kobayashi, Y. Yang, K. Hayashi, A.R. Akhmetzhanov, S. Jung, et al., Incubation Period and Other Epidemiological Characteristics of 2019 Novel Coronavirus Infections with Right Truncation: A Statistical Analysis of Publicly Available Case Data, *J. Clin. Med.*, **9** (2020), 538. https://doi.org/10.3390/jcm9020538
3. A.W. Byrne, D. McEvoy, A.B. Collins, K. Hunt, M. Casey, A. Barber, et al., Inferred duration of infectious period of SARS-CoV-2: rapid scoping review and analysis of available evidence for asymptomatic and symptomatic COVID-19 cases, *BMJ Open*, **10** (2020), e039856. https://doi.org/10.1136/bmjopen-2020-039856
4. *Ministry of Health, Labour and Welfare of Japan*, Visualizing the data: information on COVID-19 infections.
   Available from: https://covid19.mhlw.go.jp/en/
5. *Digital Agency*, Vaccination Record System (VRS).
   Available from: https://info.vrs.digital.go.jp/opendata/ (Japanese)
6. *Statistics of Japan*, Re-calculated on the complete counts of the 2020 Population Census (Oct. 2020 – June 2021).
   Available from: https://www.stat.go.jp/english/data/jinsui/2.html
7. O. Diekmann, J.A.P. Heesterbeek, J.A.J. Metz, On the definition and the computation of the basic reproduction ratio R0 in models for infectious diseases in heterogeneous populations, *J. Math. Biol.*, **28** (1990), 365–382. https://doi.org/10.1007/BF00178324

8. T. Kuniya, Numerical approximation of the basic reproduction number for a class of age-structured epidemic models, *Appl. Math. Lett.*, **73** (2017), 106-112. http://dx.doi.org/10.1016/j.aml.2017.04.031
9. S. Kodera, E.A. Rashed, A. Hirata, Estimation of real-world vaccination effectiveness of mRNA COVID-19 vaccines against delta and omicron variants in Japan, *Vaccines*, **10** (2022), 430. https://doi.org/10.3390/vaccines10030430
10. *SPI-M-O*, Summary of further modelling of easing restrictions – Roadmap Step 2 (2021). Available from: https://assets.publishing.service.gov.uk/government/uploads/system/uploads/attachment_data/file/975909/S1182_SPI-M-O_Summary_of_modelling_of_easing_roadmap_step_2_restrictions.pdf
11. *Ministry of Health, Labour and Welfare of Japan*, Life Tables. Available from: https://www.mhlw.go.jp/english/database/db-hw/vs02.html

Figures:

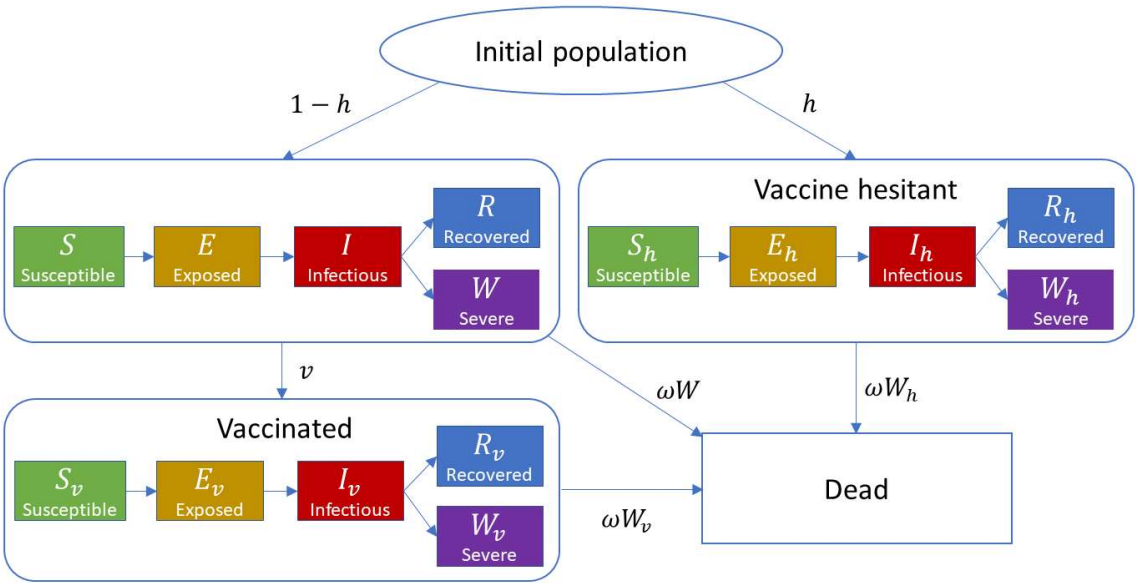

Figure S1: Transfer diagram of our model.

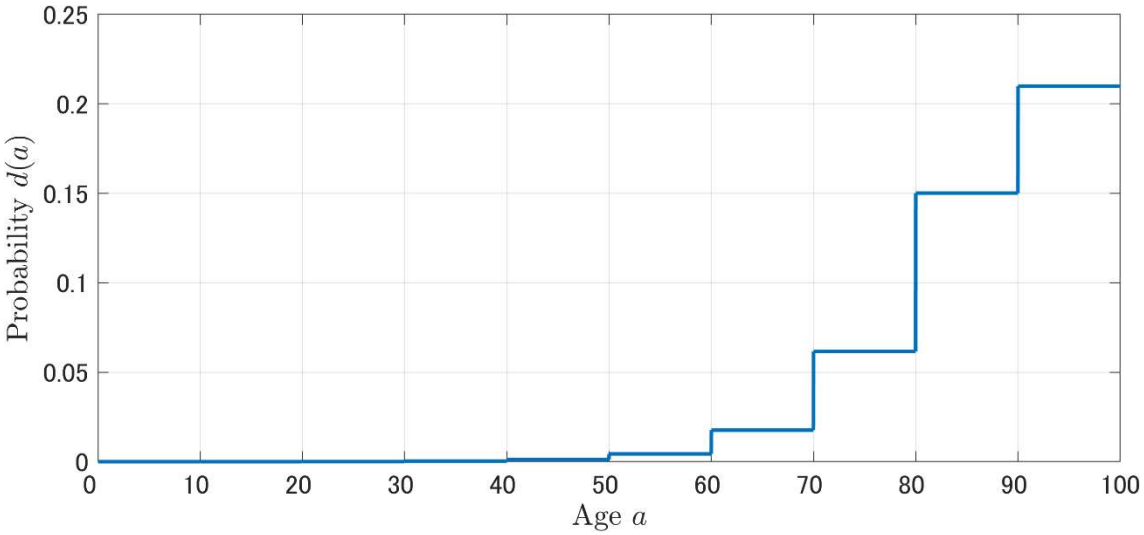

Figure S2: Age-specific probability at which a recovered individual becomes severe.

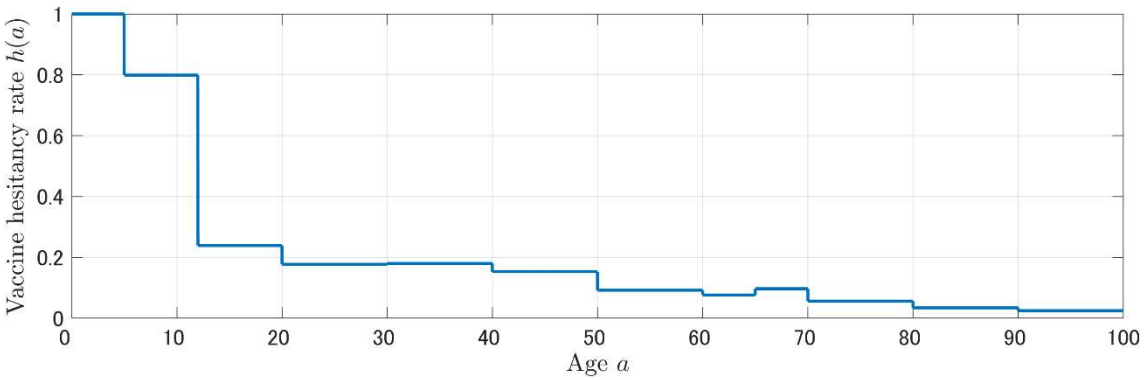

Figure S3: Age-specific vaccine hesitancy rate $h(a)$.

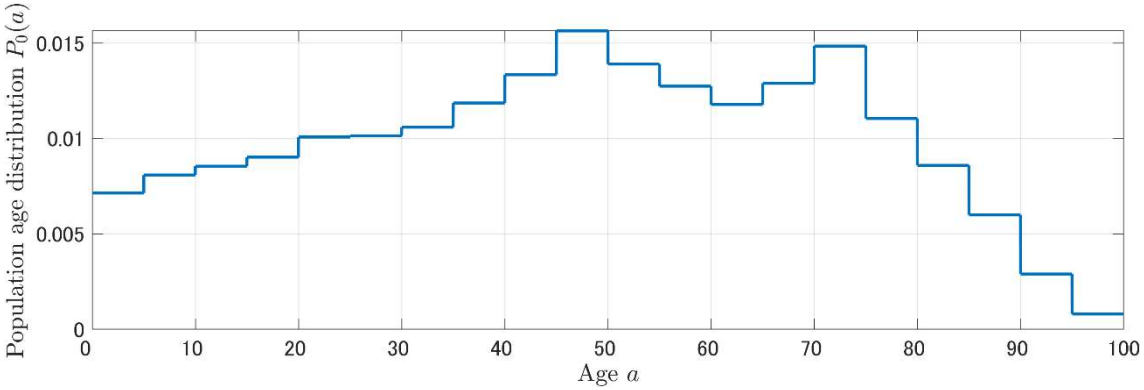

Figure S4: Initial population age distribution $P_0(a)$.

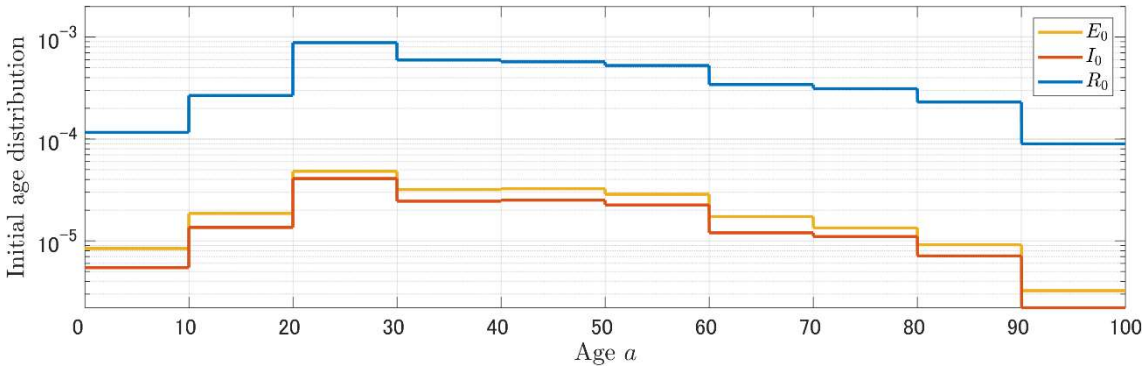

Figure S5: Initial age distributions of exposed $E_0(a)$, infectious $I_0(a)$ and recovered $R_0(a)$ populations.

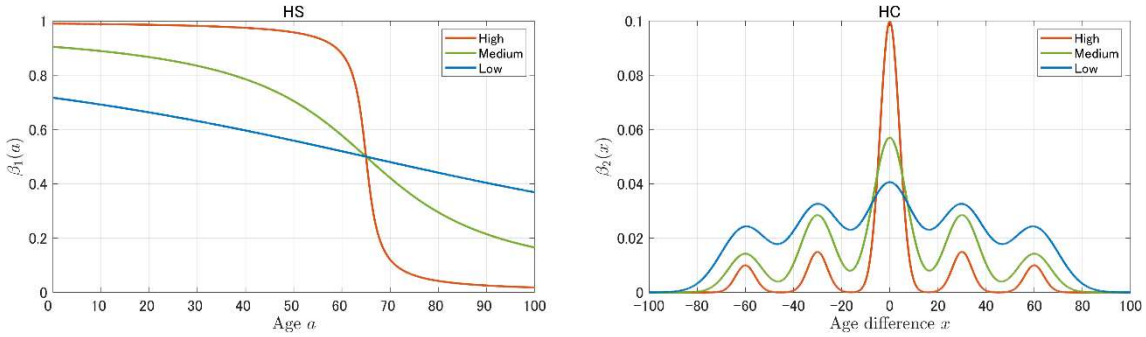

Figure S6: Age dependent susceptibility $\beta_1(a)$ (HS) and contact frequency $\beta_2(x)$ among individuals whose age difference is x (HC). Three levels of heterogeneity (high, medium and low) are considered to each of them.

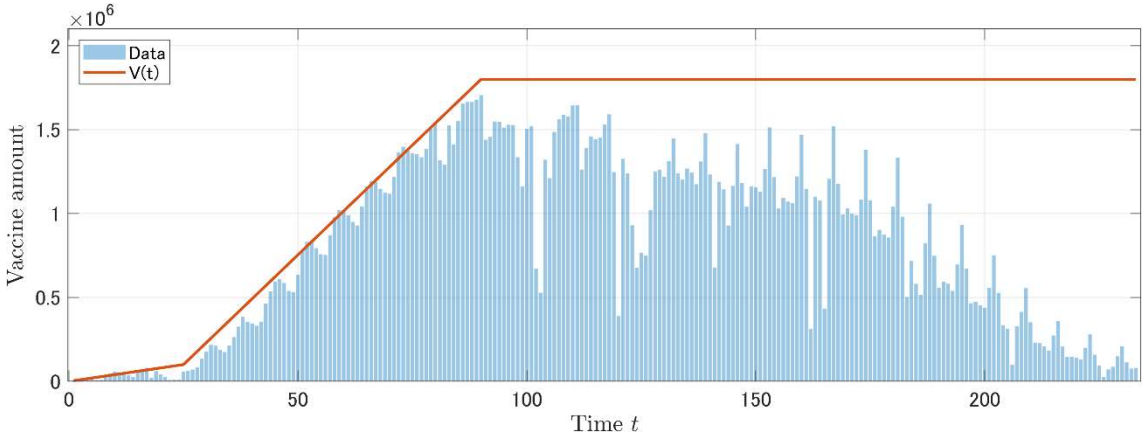

Figure S7: Daily number of vaccination shots in Japan from April 12, 2021 to November 30, 2021.

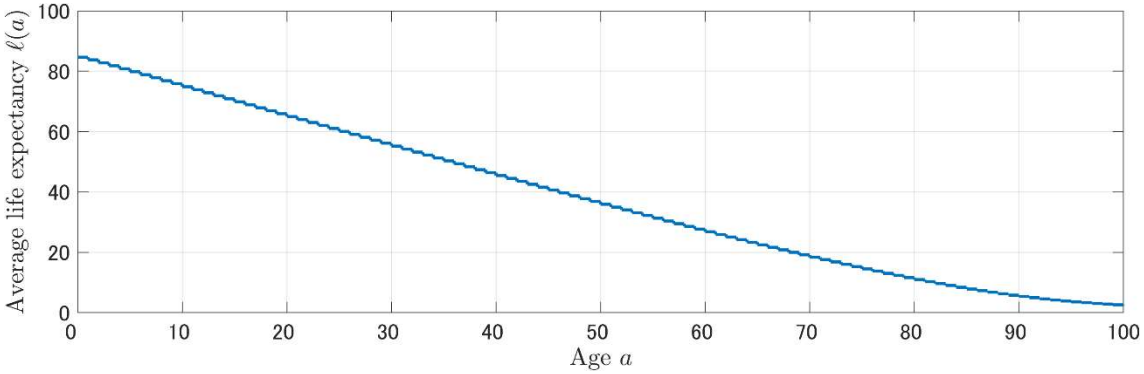

Figure S8: Age-specific average life expectancy $\ell(a)$.

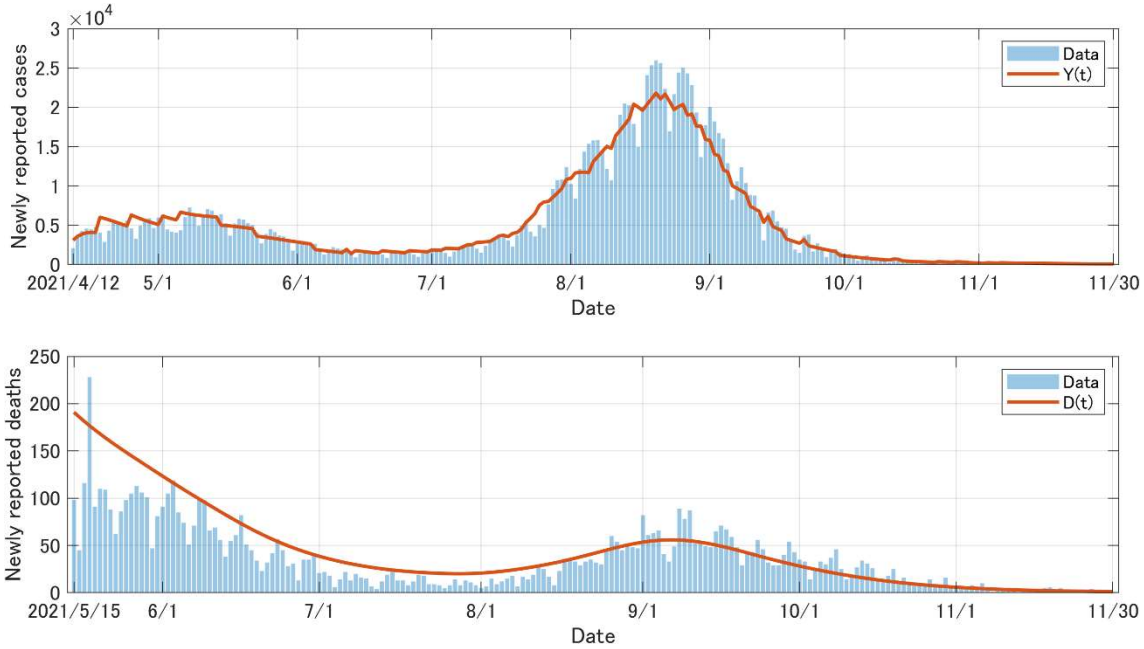

Figure S9: Daily number of newly reported cases (top) and deaths (bottom). Functions $Y(t)$ and $D(t)$ are derived from our model.

```
for t=1:1:nt-1
    for a=1:1:na
        f1(a)=Sv(t,a,T)+Ev(t,a,T)+Iv(t,a,T)+Rv(t,a,T);
        f2(a)=v2(a)*(S(t,a)+E(t,a)+I(t,a)+R(t,a));
    end
    F1=sum(f1)*da;
    F2=sum(f2)*da;
    v1(t)=max((V(t)/N-F1)/F2,0);

    for a=1:1:na
        v=v1(t)*v2(a);

        for b=1:1:na
            bI(a,b)=bet(a,b)*(I(t,b)+Ih(t,b)+sum(Iv(t,b,1:1:nx))*dx);
        end
        lam=sum(bI(a,:))*da;

        S(t+1,a)=S(t,a)+dt*(-lam*S(t,a)-v*S(t,a));
        E(t+1,a)=E(t,a)+dt*(lam*S(t,a)-eps*E(t,a)-v*E(t,a));
        I(t+1,a)=I(t,a)+dt*(eps*E(t,a)-gam*I(t,a)-v*I(t,a));
        R(t+1,a)=R(t,a)+dt*((1-d(a*da))*gam*I(t,a)-v*R(t,a));
        W(t+1,a)=W(t,a)+dt*(d(a*da)*gam*I(t,a)-om*W(t,a));

        Sh(t+1,a)=Sh(t,a)+dt*(-lam*Sh(t,a));
        Eh(t+1,a)=Eh(t,a)+dt*(lam*Sh(t,a)-eps*Eh(t,a));
        Ih(t+1,a)=Ih(t,a)+dt*(eps*Eh(t,a)-gam*Ih(t,a));
        Rh(t+1,a)=Rh(t,a)+dt*((1-d(a*da))*gam*Ih(t,a));
        Wh(t+1,a)=Wh(t,a)+dt*(d(a*da)*gam*Ih(t,a)-om*Wh(t,a));

        Sv(t+1,a,1)=v*S(t,a);
        Ev(t+1,a,1)=v*E(t,a);
        Iv(t+1,a,1)=v*I(t,a);
        Rv(t+1,a,1)=v*R(t,a);

        SS(1)=(1-Sig(1))*lam*Sv(t,a,1);
        for x=2:1:nx
            Sv(t+1,a,x)=Sv(t,a,x)+dt*(-(Sv(t,a,x)-Sv(t,a,x-1))/dx...
                -(1-Sig(x))*lam*Sv(t,a,x-1));
            Ev(t+1,a,x)=Ev(t,a,x)+dt*(-(Ev(t,a,x)-Ev(t,a,x-1))/dx...
                +(1-Sig(x))*lam*Sv(t,a,x-1)-eps*Ev(t,a,x-1));
            Iv(t+1,a,x)=Iv(t,a,x)+dt*(-(Iv(t,a,x)-Iv(t,a,x-1))/dx...
                +eps*Ev(t,a,x-1)-gam*Iv(t,a,x-1));
            Rv(t+1,a,x)=Rv(t,a,x)+dt*(-(Rv(t,a,x)-Rv(t,a,x-1))/dx...
                +(1-(1-Del(x))*d(a))*gam*Iv(t,a,x-1));
            WW(x)=(1-Del(x))*d(a)*gam*Iv(t,a,x-1);
            SS(x)=(1-Sig(x))*lam*Sv(t,a,x);
        end
    end
end
```

Figure S10: The main part of our simulation code for MATLAB. Some symbols are defined in other parts or files.

Table

Table S1: The parameter values in our model.

Symbol	Meaning	Value	Unit	Reference
t	Time	0 – 232	day	-
a	Age	0 – 100	year	-
τ	Vaccine age	0 – 232	day	-
$v(t,a)$	Vaccination rate	(1)	day^{-1}	[5]
ε	Transition rate from exposed to infectious	0.2	day^{-1}	[1,2]
γ	Removal rate	0.1	day^{-1}	[3]
$d(a)$	Probability at which an infected individual becomes severe	Figure S2	percent $\times 10^{-2}$	[4]
ω	Mortality rate of severe individuals	0.1	day^{-1}	Assumed
$\sigma(\tau)$	Vaccine efficacy in reducing the risk of infection	(2)	percent $\times 10^{-2}$	[9,10]
$\delta(\tau)$	Vaccine efficacy in reducing the risk of death	(2)	percent $\times 10^{-2}$	[9,10]
$h(a)$	Vaccine hesitancy rate	Figure S3	percent $\times 10^{-2}$	[5]
$\ell(a)$	Average life expectancy	Figure S8	Year	[11]
κ	Infection transmission rate	Determined according to $\mathcal{R}_0$	-	Assumed
$\beta_1(a)$	Age dependent susceptibility	Figure S6	-	Assumed
$\beta_2(x)$	Contact frequency among individuals whose age difference is x	Figure S6	-	Assumed
N	Total population in Japan	1.26×10^8	person	[6]
χ	Detection ratio	0.5	percent $\times 10^{-2}$	Assumed